Journal of Neuroscience Research 81:102–109 (2005)

Deafness-Related Decreases in Glycine-Immunoreactive Labeling in the Rat Cochlear Nucleus

Mikiya Asako,[1,2] Avril G. Holt,[1] Ronald D. Griffith,[1] Eric D. Buras,[1] and Richard A. Altschuler[1,3]★

[1]Kresge Hearing Research Institute, Department of Otolaryngology/Head Neck Surgery, University of Michigan, Ann Arbor, Michigan
[2]Department of Otolaryngology/Head Neck Surgery, Kansai Medical University, Osaka, Japan
[3]Department of Cell and Developmental Biology, University of Michigan, Ann Arbor, Michigan

There is increasing evidence of activity-related plasticity in auditory pathways. The present study examined the effects of decreased activity on immunolocalization of the inhibitory neurotransmitter glycine in the cochlear nucleus of the rat after bilateral cochlear ablation. Specifically, glycine-immunoreactive puncta adjacent to somatic profiles were compared in normal hearing animals and animals deafened for 14 days. The number of glycine-immunoreactive puncta surrounding somatic profiles of spherical and globular bushy cells, glycine-immunoreactive type I stellate multipolar cells, radiate neurons (type II stellate multipolar cells), and fusiform cells decreased significantly. In addition, the number of glycine immunopositive tuberculoventral (vertical or corn) cells in the deep layer of the dorsal cochlear nucleus also decreased significantly. These results suggest that decreased inhibition reported in cochlear nucleus after deafness may be due to decreases in glycine.

Key words: hearing; auditory; ablation; neurotransmitter

There is increasing evidence of plasticity in the mature auditory system, with decreased activity from deafness or increased activity from noise overstimulation capable of inducing marked changes (recently reviewed by Syka, 2002). Activity-induced changes in the auditory brain stem range from changes in gene expression (e.g., Holt et al., 2005) to changes in neuronal response profiles (Francis and Manis, 2000). One of the most striking deafness-related changes in the auditory brain stem is a decrease in inhibition and an increase in spontaneous or evoked excitation, found in both the inferior colliculus (IC) and the cochlear nucleus (CN; Gerken, 1979; Willott and Lu, 1982; Bledsoe et al., 1995; Kaltenbach, 2000; Mossop et al., 2000; Salvi et al., 2000; Willott and Turner, 2000; Shaddock Palombi et al., 2001), often leading to a change in the tonotopic map (Leake et al., 2000; Nagase et al., 2000; Snyder et al., 2000). In the IC, the decreased inhibition seems associated with decreases in the inhibitory amino acid neurotransmitter γ-aminobutyric acid (GABA), with studies showing decreased GABA release (Bledsoe et al., 1995) and decreases in the GABA-synthesizing enzyme glutamic acid decarboxylase (GAD) as well as GABA binding (Bauer et al., 2000; Milbrandt et al., 2000; Mossop et al., 2000; Caspary et al., 2002). In the CN, however, many studies suggest that glycine is the major inhibitory transmitter (Altschuler et al., 1986; Wu and Oertel, 1986; Caspary et al., 1987, 1994; Wenthold et al., 1987; Adams and Mugnaini, 1990; Bledsoe et al., 1990; Wickesberg and Oertel, 1990; Helfert et al., 1992; Kolston et al., 1992; Kuwabara and Zook, 1992, 1999; Grothe and Sanes, 1993; Wickesberg et al., 1994; Wu and Kelly, 1994; Sato et al., 1995; Golding and Oertel, 1996; Juiz et al., 1996; Harty and Manis, 1998; Doucet et al., 1999; Godfrey et al., 2000; Zheng et al., 2000). Decreases in glycine-immunoreactive neurons and puncta (Willott et al., 1993; Willott and Turner, 2000) and changes in glycine receptor subunits (Krenning et al., 1998) are associated with age-related hearing loss. Glycine release, glycine uptake, and glycine receptor binding all change after cochlear ablation (Suneja et al., 1998a,b; Potashner et al., 2000). Because glycine is implicated in deafness-related decreases in inhibition within the CN, then decreased glycine levels might also be expected in the CN. We therefore addressed whether there are deafness-related decreases in glycine immunoreactivity within the cochlear nucleus 14 days after deafness. The 14-day point after deafness was chosen because marked decreases in the release of GABA have been observed in the

Contract grant sponsor: NIH/NIDCD; Contract grant number: 00383; Contract grant sponsor: NIH; Contract grant number: 1F32GM013553; Contract grant sponsor: NIDCD; Contract grant number: P30 DC05188.

★Correspondence to: Richard A Altschuler, KHRI, University of Michigan, 1301 East Ann, Ann Arbor, MI 48109-0506.
E-mail: shuler@umich.edu

Received 26 May 2004; Revised 24 March 2005; Accepted 29 March 2005

Published online 31 May 2005 in Wiley InterScience (www.interscience.wiley.com). DOI: 10.1002/jnr.20542

inferior colliculus at this time after deafness (Bledsoe et al., 1995, 1997).

MATERIALS AND METHODS

Animals and Surgical procedures

All animals used in this study were female Sprague-Dawley rats weighing between 200–300 g and were obtained from Charles River Laboratories. The experimental group of rats was bilaterally deafened via introduction of neomycin through each round window. This deafened group ($n = 5$) was assessed 14 days after deafening. The animals in the control group ($n = 5$) were age matched and had normal hearing based on auditory brain stem response (ABR) measures. Each rat in the deafened group was anesthetized with intramuscular injections of xylazine (8 mg/kg) and ketamine (75 mg/kg). Local injections of 1% lidocaine-HCl solution were also made at the site of each surgical incision (subcutaneous). Surgical procedures were carried out under aseptic conditions. The skin incision was made through the postauricular region of the lateral neck. The bulla was exposed without resection of any major muscles. A small defect in the bulla was opened and 30 μl of 30% neomycin were injected over 3 min through the round window using a Hamilton syringe. The skin incision was then closed with sutures. After surgery, animal were injected with sterile 0.9% sodium chloride solution and allowed to recover under a heating lamp.

Hearing Loss Assessment

Hearing was assessed by auditory brain stem response (ABR) measures at 2, 10, and 20 kHz in all animals at the beginning of the study and only those with normal hearing were included in the study. A second measure of hearing was done 14 days after the deafening, for animals in the deafness group. An 80-dB shift from the normal control threshold averaged across the three frequencies was considered necessary for continued inclusion in the deafness group.

Tissue Processing

All rats were deeply anesthetized with a single intraperitoneal dose of 350 mg/kg of chloral hydrate and then perfused transcardially with 30 ml of 0.12 M phosphate buffered saline (PBS; pH 7.4), followed immediately by 300 ml mixed aldehyde fixative containing 2% paraformaldehyde and 1.25% glutaraldehyde in 0.12 M phosphate buffer. Animals were decapitated and brains were carefully removed from the cranium and then immersed in the same fixative for 90 min at 4°C for post fixation. After an 8–14-hr rinse in PBS, the lower brain stem (medulla and pons) was dissected and glued onto a chuck. Coronal sections (150 μm) containing the CN were cut with a vibrating microtome (Vibratome). Slices were chosen that contained a predefined (based on anatomic landmarks and cytoarchitectural features), consistent, region of interest (ROI) in the anteroventral cochlear nucleus (AVCN), posteroventral cochlear nucleus (PVCN), or the dorsal cochlear nucleus (DCN). These sections were placed in 1% OsO_4 in phosphate buffer for 45 min. This was followed by a rinse in phosphate buffer, incubation for 1 hr in 2% uranyl acetate, and another phosphate buffer rinse. Sections were then dehydrated through a graded series of ethanol and then infiltrated through graded mixtures of EPON 812 and propylene oxide. After 4 hr in 100% EPON 812, sections were placed between plastic sheets and polymerized for 48 hr at 60°C. Sections were viewed under a Leica dissecting microscope. For each animal assessed, an area containing the ROIs (AVCN, PVCN, and DCN) was cut out of the specific sections in which they were present and glued onto an ultramicrotome chuck. Serial 1-μm semithin sections were then cut through the ROI on a Reichert ultramicrotome. Systematic random sampling (Coggeshall and Lekan, 1996) was utilized, where the starting point for a series were random with the next sections in the series and then assessed at fixed intervals. Five 1-μm sections (separated by 12 μm; the 1st, 13th, 25th, 37th, and 49th in each series once the start point was selected) from each rat were processed for immunocytochemistry and quantitative analysis. Five adjacent 1-μm sections (the 2nd, 14th, 26th, 39th and 50th in the series) received a Nissl stain (toluidine blue) for anatomic reference.

Immunocytochemistry

Sections were etched for 40 min in sodium ethoxide, rehydrated, and then treated in 1% sodium periodate for 10 min. Postembedding immunocytochemistry was then carried out. Sections were incubated 4°C for 40 hr in rabbit anti-glycine antibody IgG (Chemicon, Temecula, CA) diluted 1:1,200 in 0.5 M Tris buffer containing 5.0% normal goat serum. After thorough rinsing in Tris buffer, sequential incubations were carried out after using the Vectastain procedure (biotinylated goat anti-rabbit IgG diluted 1:100 in 0.5 M Tris buffer containing 5.0% normal goat serum; avidin-biotin-peroxidase complex [ABC Kit], diluted in 0.5 M Tris buffer). Sections were then treated for 3 min in 0.05% diaminobenzidine (DAB) in 0.01% H_2O_2 to visualize the reaction product. The DAB reaction was then stopped rapidly by rinsing several times with double-distilled water. Sections were then dried, dehydrated, and coverslipped.

Image Acquisition

Five sections each from five rats in each group were used for AVCN, PVCN, and DCN assessments. Digital images were acquired with a Spot camera (Diagnostic Instruments, Inc.) on a Zeiss Axioscop2 photomicroscope and assessed quantitatively using MetaMorph (Universal Imaging) software. A grayscale image from each ROI on a section was acquired using the CCD camera while holding all image-gathering parameters constant. Cells types were differentiated based on the size, shape, and location criteria of Cant and Morest (Cant and Morest, 1979a,b; Cant, 1981) as well as glycine-immunoreactive staining. A somatic profile of a neuron needed to contain a nucleus to be assessed. Because nuclei are no larger than the 12-μm interval between sections, this ensured that the same neuron would be not assessed twice. Every neuron with an identifiable nucleus was assessed within each predefined ROI. The somatic profile of each neuron with a nucleus was circled and the area, perimeter, and shape of the neurons were entered automatically into a spreadsheet program. Positive immunostaining was defined as intensity at least 7× over background and positive

Fig. 1. Glycine immunoreactivity in the dorsal cochlear nucleus (DCN). The molecular, fusiform and deep layers of the DCN contain many glycine-immunolabeled puncta. As expected, the cartwheel cells in the molecular layer are glycine immunopositive. The fusiform neurons in the fusiform layer are immunonegative for glycine. Mol, molecular layer; Fus, fusiform layer; Deep, deep layer. Scale bar = 25 μm.

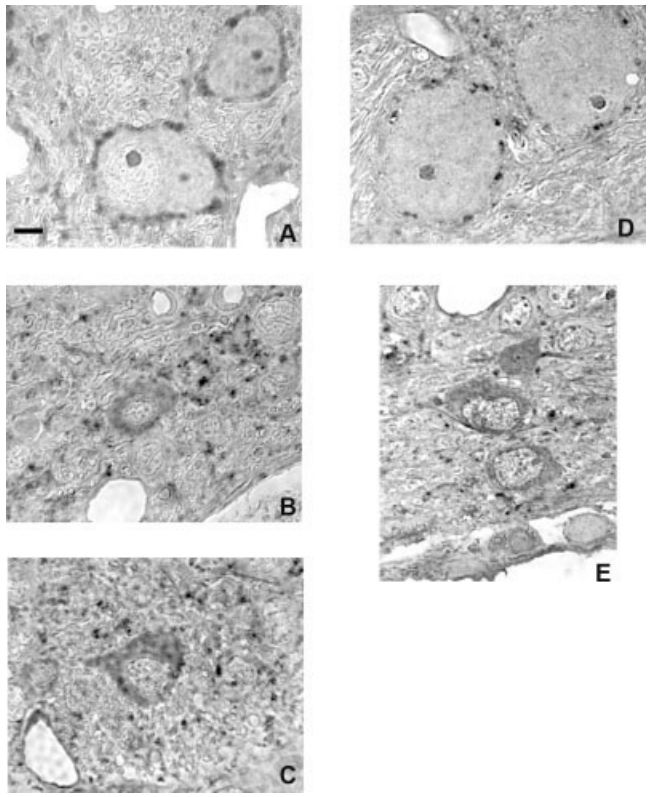

Fig. 2. Glycine immunoreactivity in the ventral cochlear nucleus in normal hearing rats (**A–C**) and in rats 14 days after bilateral deafening (**D, E**). Glycine immunolabeling decreases in intensity and in the number of axosomatic puncta on most cell types 14 days after deafness. Scale bar = 5 μm.

puncta were defined further by size constraints (1.0–4.5 μm^2) and shape (round to oval) criteria. The number of glycine-immunoreactive puncta directly apposing each circled somatic profile was then determined and entered into the spreadsheet program. Additionally, the number of immunopositive tuberculoventral cells within the deep layer of the DCN was also determined in DCN sections.

Statistical Analyses

Analysis of variance (ANOVA) was carried out using StatView software. Comparison between normal hearing and deafened groups was made for axosomatic puncta and for the cell area for each cell type from each of 25 sections assessed in each group. The average was calculated per animal, with degrees of freedom (*df*) equal to 1 in the numerator (deaf vs. normal) and 8 in the denominator (five animals per group) with a confidence level of 95% necessary for significance. A Scheffe multiple comparison test was used for post-hoc comparisons.

RESULTS

Glycine Immunoreactivity: Normal

Glycine-immunoreactive staining in the CN of normal hearing rats (Fig. 1 and 2) was consistent with the results of previous studies (Altschuler et al., 1986; Wenthold, 1987; Wenthold et al., 1987; Wickesberg and Oertel, 1990; Kolston et al., 1992; Wickesberg et al., 1994; Juiz et al., 1996; Doucet et al., 1999). Most neurons in the VCN were not immunostained for glycine; however, glycine-immunoreactive radiate neurons (type II stellate multipolar cells; Doucet and Ryugo, 1997; Doucet et al., 1999) and smaller glycine-immunoreactive type I stellate multipolar cells were found throughout the magnocellular area of the VCN. Almost all neurons in the magnocellular region of the VCN had glycine-immunoreactive puncta on their somata. These ranged from few on the soma of type I stellate multipolar cells to numerous on the soma of spherical and globular bushy cells. In the DCN (Fig. 1), many glycine-immunostained cells were found in the molecular layer and glycine-immunostained tuberculoventral (vertical, corn) cells (Wickesberg et al., 1991, 1994) were in the deep layer. Numerous glycine-immunoreactive axosomatic puncta were found on fusiform cells of the fusiform layer.

Deafness-Related Changes in CN

Because there was also a decrease in the area of somatic profiles for most CN cell types after deafness, an increase in the density of glycine-immunostained axosomatic puncta could theoretically result as the area they could contact shrinks, with an ''artificial'' increase in their number per somatic profile. The present study, however, found marked decreases after deafening in the

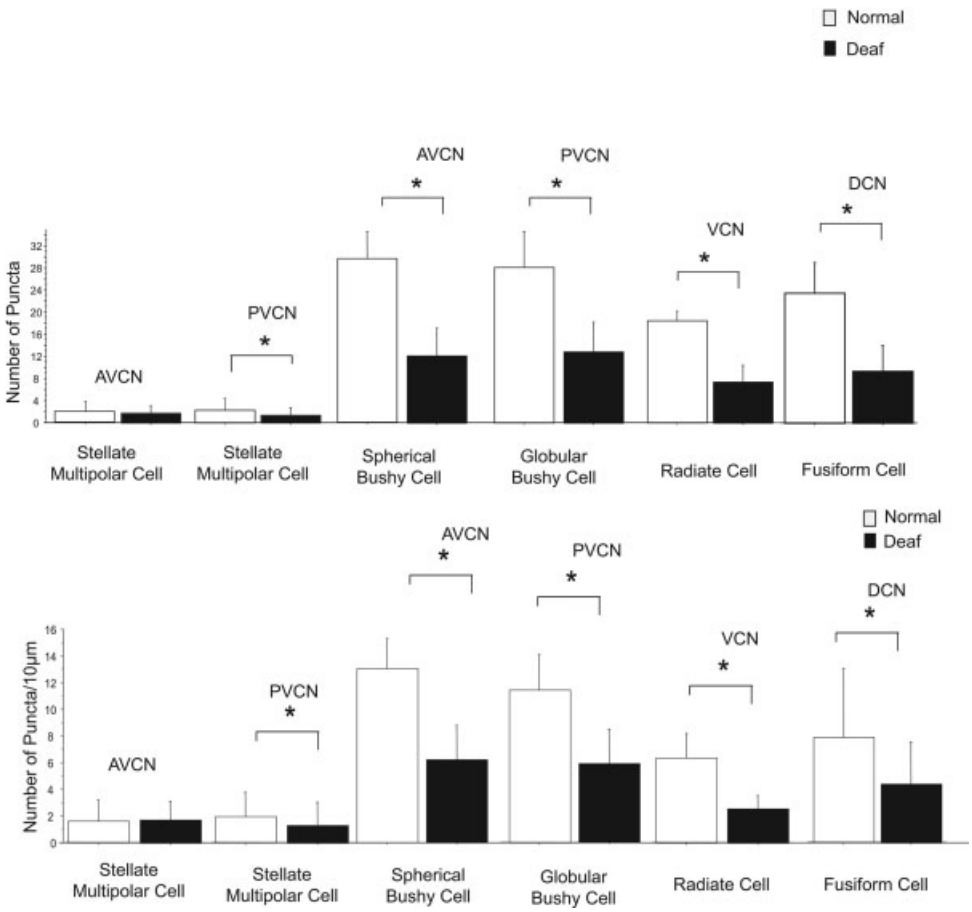

Fig. 3. Differences in the number of glycine-immunoreactive axosomatic puncta on different cell types in the cochlear nucleus (CN) between normal hearing rats (white bars) and rats 14 days after bilateral deafening (black bars). Data are expressed as the number of labeled puncta on a somatic profile (top) and as the number of puncta per 10 μm of somatic profile (bottom). Significant (*$P \leq 0.05$) decreases are seen for glycine-immunoreactive type I stellate multipolar cells in posteroventral CN (PVCN), spherical bushy cells, globular bushy cells, radiate cells (type II stellate multipolar cells) and fusiform cells, but not glycine-immunoreactive type I stellate multipolar cells in anteroventral CN (AVCN). Error bars represent ±1 standard deviation.

number of glycine-immunostained axosomatic puncta considered either as the total per somatic profile or the number per 10 μm of somatic profile. Whatever effect the change in cell size might have had was overcome by the magnitude of the decrease in labeled puncta. There was also a decrease in the number of glycine-immunostained tuberculoventral cells in the deep layer of the DCN.

Spherical bushy cells. Spherical bushy cells (normal, $n = 145$; deaf, $n = 199$) were located in the AVCN and were not immunostained for glycine. They were spherical in shape, large (>250 μm^2), and received large numbers (>20) of glycine-immunopositive axosomatic puncta on a somatic profile. The number of axosomatic glycine-immunoreactive puncta per somatic profile for spherical bushy cells was 39.5 ± 4.9 in normal hearing animals. In animals that were deaf for 14 days, there was a significant ($P \leq 0.01$) 59% decrease to 12.1 ± 5.0 (Fig. 2 and 3). The decrease was 53% (significant, $P \leq 0.01$) when expressed as the number of puncta per 10 μm of somatic profile, going from 13.0 ± 2.2 in normal hearing animals to 6.2 ± 2.6 after deafening (Fig. 3).

Spherical bushy cells had an average area of 347.9 ± 66.9 μm^2 in the AVCN of normal hearing animals. Fourteen days after deafness there was a significant ($P \leq 0.01$) 21% decrease in average area to 274.3 ± 67.9 μm^2 (Fig. 4), comparable to what has been described previously (Pasic and Rubel, 1989, 1991; Pasic et al., 1994; Lesperance et al., 1995; Winsky and Jacobowitz, 1995; Nishiyama et al., 2000).

Globular bushy cells. Globular bushy cells were located in the PVCN (Fig. 2A,B) and were not immunostained for glycine (normal, $n = 165$; deaf, $n = 235$). They were spherical in shape, large (>250 μm^2) and received large numbers (>20) of glycine-immunopositive axosomatic puncta on a somatic profile. The number of axosomatic glycine-immunoreactive puncta per

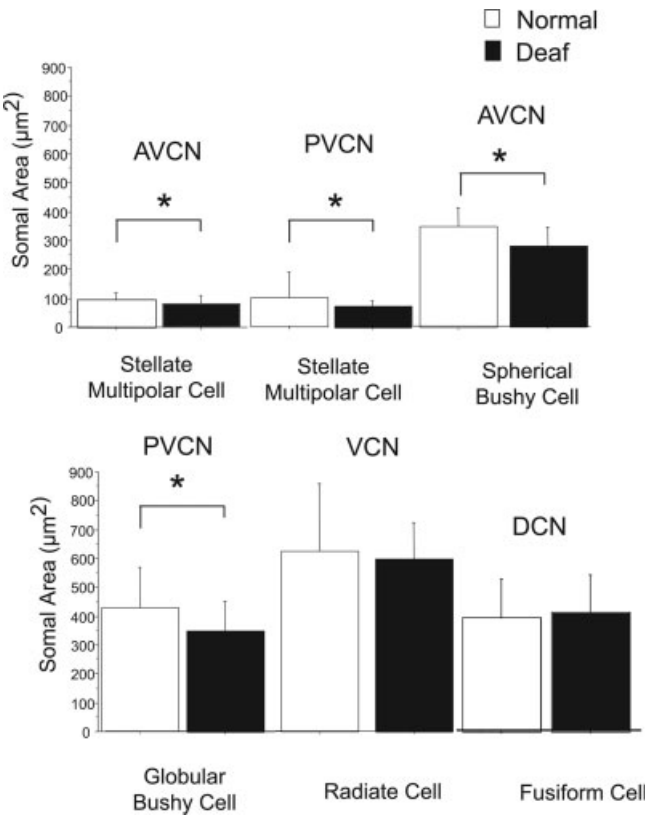

Fig. 4. Changes in cell size in the cochlear nucleus (CN) of normal hearing rats (white bars) vs. that in rats 14 days after deafness (black bars). Significant (*$P \leq 0.05$) decreases are seen in glycine-immunoreactive type I stellate multipolar cells, spherical bushy cells and globular bushy cells, but not radiate cells (type II stellate multipolar cells) or fusiform cells. Error bars represent ±1 standard deviation. AVCN, anteroventral CN; PVCN, posteroventral CN; VCN, ventral CN; DCN, dorsal CN.

somatic profile for globular bushy cells was 28.2 ± 6.5 in normal hearing animals. In animals that were deaf for 14 days, there was a significant ($P \leq 0.01$) 55% decrease to 12.8 ± 5.5 (Fig. 2B and 3). When expressed as the number of puncta per 10 μm of somatic profile, there was a significant ($P \leq 0.01$) 49% decrease from 11.4 ± 2.6 to 5.9 ± 2.5.

Globular bushy cells in PVCN showed a significant ($P \leq 0.01$) decrease from an average area of 424.5 ± 144.8 μm^2 in the CN of normal hearing animals to an average area of 346.3 ± 104.1 μm^2 14 days after deafness (Fig. 2 and 4).

Radiate cells (type II stellate multipolar cells). Radiate cells were found in the AVCN and PVCN (Fig. 2D,E) and were glycine immunopositive (normal, $n = 4$; deaf, $n = 4$). They were spherical in shape, large (>350 μm^2), and received large numbers (>20) of immunopositive axosomatic puncta per somatic profile. The number of axosomatic glycine-immunoreactive puncta per somatic profile for radiate cells was 18.5 ± 1.7 in normal hearing animals, whereas in animals that were deaf for 14 days, there was a significant ($P \leq 0.01$) 61% decrease to 7.3 ± 3.2 (Fig. 2 and 3). When expressed as the number of puncta per 10 μm of somatic profile, there was the same significant ($P \leq 0.01$) 61% decrease, now from 6.4 ± 1.8 to 2.5 ± 1.0. Radiate cells had an average area of 624.1 ± 233.2 μm^2 in the CN of normal hearing animals and did not show significant decrease in area after deafening (593.8 ± 127.1 μm^2; Fig. 2D,E and 4).

Glycine-immunoreactive type I stellate multipolar cells. Glycine-immunoreactive type I stellate multipolar cells (Fig. 2C,E) were assessed in both the AVCN (normal, $n = 72$; deaf, $n = 47$), and PVCN (normal, $n = 97$; deaf, $n = 117$). They were small in size (<150 μm^2) and received few (<5) immunopositive puncta. In the AVCN, there was not a significant deafness-related decrease in the number of axosomatic glycine-immunoreactive puncta per somatic profile 14 days after deafening. There were 1.8 ± 1.9 in normal hearing animals and 1.7 ± 1.4 at 14 days after deafening. In PVCN, however, these cells exhibited a 45% decrease from 2.2 ± 2.2 in normal hearing animals to 1.2 ± 1.5 14 days after deafening ($P \leq 0.01$; (Fig. 2 and 3). Results were similar, when considered as the number of puncta per 10 μm of somatic profile, staying at 1.6 in AVCN and decreasing 34% in PVCN ($P \leq 0.01$) from 1.8 ± 1.8 to 1.2 ± 1.7.

Glycine-immunoreactive type I stellate multipolar cells had an average area of 89.6 ± 26.0 μm^2 in the AVCN of normal hearing animals. Fourteen days after deafness, there was a significant ($P \leq 0.05$) decrease to an average area of 78.9 ± 26.6 μm^2. In the PVCN, these cells in were slightly larger 98.1 ± 90.2 μm^2 and their decrease after 14 days of deafness to 69.8 ± 20.3 μm^2 was significant ($P \leq 0.01$; Fig. 4).

Fusiform cells. Fusiform cells in the fusiform layer of the DCN (Fig. 1) were large (>250 μm^2), fusiform shaped, and were not immunostained for glycine (normal, $n = 71$; deaf, $n = 93$). The number of axosomatic glycine-immunoreactive puncta per somatic profile for fusiform cells was 23.6 ± 5.7 in normal hearing animals. After 14 days of deafness, there was a significant ($P \leq 0.01$) 60% decrease to 9.3 ± 4.9 (Fig. 3). When expressed as the number of puncta per 10 μm of somatic profile, there was a significant ($P \leq 0.01$) 45% decrease from 7.8 ± 5.2 in normal hearing animals to 4.3 ± 3.2 in animals 14 days after deafening.

Fusiform cells of the DCN did not show a significant deafness-related change in cell size, with an area of 390.8 ± 132.0 μm^2 in normal hearing animals and 406.5 ± 132.8 μm^2 in animals 14 days after deafening (Fig. 4).

Tuberculoventral cells (vertical cells and corn cells). Tuberculoventral cells were small in size, glycine immunopositive, and in the deep layer of the DCN. The number of glycine immunopositive tuberculoventral cells per 1,000 μm^2 in the deep layer of the DCN decreased 42% from 81 ± 21.0 in normal hearing animal to 47 ± 19.0 in animals 14 days after deafening (Fig. 5). The tuberculoventral cells (normal, $n = 112$;

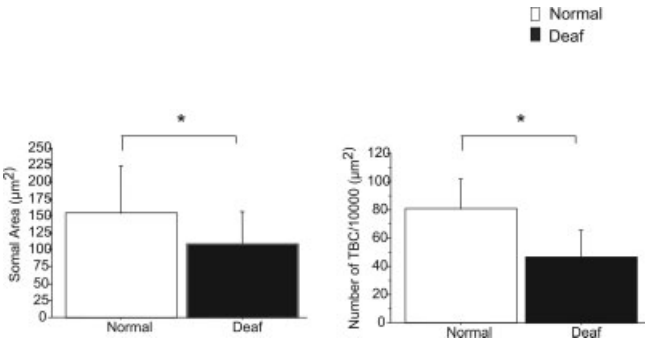

Fig. 5. Differences in the size of tuberculoventral cells (TBC) in the deep layer of the dorsal cochlear nucleus (DCN) when comparing normal hearing rats (white bars) and rats 14 days after bilateral deafening (black bars), as well as the number of glycine-immunoreactive TBC per 1,000 μm^2. A significant decrease was seen both in cell size and in the number of glycine-immunopositive cells per 1,000 μm^2. Error bars represent ± 1 standard deviation. $^*P \leq 0.05$.

deaf, $n = 62$) also decreased significantly ($P \leq 0.01$) in size from an average area of 154.0 $\pm$ 70.1 μm^2 in normal hearing animals to 108.6 $\pm$ 47.1 μm^2 in animals 14 days after deafness (Fig. 5).

DISCUSSION

The results of this study show marked changes in the number of glycine-immunoreactive puncta on spherical bushy, globular bushy, radiate, and fusiform cells 14 days after bilateral deafening. This result is consistent with a loss of inhibition in the CN after deafness and decreases in glycine with age-related hearing loss (Willott et al., 1993; Willott and Turner, 2000) and cochlear ablation (Suneja et al., 1998a,b; Potashner et al., 2000). The latter studies (Suneja et al., 1998a,b; Potashner et al., 2000) reported decreases in glycine release after cochlear ablation in the AVCN and DCN but not the PVCN.

Our results showed decreases in glycine-immunolabeled puncta on neurons in all three divisions. This may correlate with decreases in the level of glycine within terminals (bringing it below the level of detection), with a physical loss of glycine-containing terminals making somatic contact, or some combination of the two. Ultrastructural studies (Bilak et al., 1997; Bendiske and Morest, 2004; Kim et al., 2004a,b,c; Subramani and Morest, 2004) and studies using synaptophysin to label terminals (Muly et al., 2002) demonstrate that there can be marked changes in terminals and synapses in the CN after deafening from noise overstimulation. Moreover, decreases in glycine levels, if they do occur, may not always correlate with decreases in release and the specific mechanisms that regulate release. Indeed deafness-related changes in potential regulators of transmitter release have been demonstrated recently in the auditory brainstem (Suneja and Potashner, 2003; Zhang et al., 2003). Immunocytochemical studies at the ultrastructural level after cochlear ablation would therefore be valuable.

There were many glycine-immunoreactive puncta in the neuropil, in addition to those apposing neuronal somata that were assessed in the current study. The immunolabeled puncta in neuropil likely correspond to axodendritic terminals containing glycine. Because we could not easily attribute these puncta to a specific neuronal type, we did not assess their number or determine if that changed after deafening. Qualitatively, however, there did seem to be a decrease in their number and the intensity of their immunostaining, suggesting that they may change as well, in a similar fashion to those on the neuronal somata.

CN neurons receive glycinergic input from multiple sources, including the DCN (Wickesberg et al., 1991, 1994; Zhang and Oertel, 1993), the contralateral VCN (Wenthold, 1987; Babalian et al., 2002), and the superior olivary complex (e.g., Ostapoff et al., 1997). It is interesting to consider whether the decrease in glycine immunostained puncta on CN neurons reflects the loss of an input from a single source or a decrease across multiple inputs. The decrease in glycine-immunostained tuberculoventral cells suggests that they may contribute to the loss of glycine-immunostained puncta in the VCN. It will be valuable in future studies to combine tract tracing and immunocytochemistry to identify further the glycine inputs that are most affected.

Spherical bushy, globular bushy, glycine-immunoreactive type I stellate multipolar and tuberculoventral cells all showed decreases in size after deafening, consistent with previous studies from our lab and others (Lesperance et al., 1995; Pasic et al., 1994; Pasic and Rubel 1991). The lack of a cell size change for fusiform cells may be related to their excitatory input from granule cells of the shell region, which may be less affected by the deafening. Another interesting question to consider is why radiate cells did not show a cell size decrease and suggests they might also have an alternate source of excitatory input.

With the results of Potashner et al. (2000) and Suneja et al. (1998a,b) showing decreases in strychnine binding in the AVCN and PVCN after cochlear ablation, it would be interesting in future studies to compare and contrast changes in glycine with changes in glycine receptors as well as comparing and contrasting changes in GABA and GABA receptors.

REFERENCES

Adams JC, Mugnaini E. 1990. Immunocytochemical evidence for inhibitory and disinhibitory circuits in the superior olive. Hear Res 49:281–298.

Altschuler RA, Betz H, Parakkal MH, Reeks KA, Wenthold RJ. 1986. Identification of glycinergic synapses in the cochlear nucleus through immunocytochemical localization of the postsynaptic receptor. Brain Res 369:316–320.

Babalian AL, Jacomme AV, Doucet JR, Ryugo DK, Rouiller EM. 2002. Commissural glycinergic inhibition of bushy and stellate cells in the anteroventral cochlear nucleus. Neuroreport 13:555–558.

Bauer CA, Brozoski TJ, Holder TM, Caspary DM. 2000. Effects of chronic salicylate on GABAergic activity in rat inferior colliculus. Hear Res 147:175–182.

Bendiske J, Morest DK. 2004. Plastic changes in synaptic vesicle distribution in the cochlear nucleus following noise exposure in mice. Assoc Res Otolaryngol Abs: p 300.

Bilak M, Kim J, Potashner SJ, Bohne BA, Morest DK. 1997. New growth of axons in the cochlear nucleus of adult chinchillas after acoustic trauma. Exp Neurol 147:256–268.

Bledsoe SC Jr, Nagase S, Altschuler RA, Miller JM. 1997. Changes in the central auditory system with deafness and return of activity via a cochlear prosthesis. In: Syka J, editor. Acoustical signal processing in the central auditory system. New York: Plenum Press. p 513–527.

Bledsoe SC Jr, Nagase S, Miller JM, Altschuler RA. 1995. Deafness-induced plasticity in the mature central auditory system. Neuroreport 7: 225–229.

Bledsoe SC Jr, Snead CR, Helfert RH, Prasad V, Wenthold RJ, Altschuler RA. 1990. Immunocytochemical and lesion studies support the hypothesis that the projection from the medial nucleus of the trapezoid body to the lateral superior olive is glycinergic. Brain Res 517:189–194.

Cant NB. 1981. The fine structure of two types of stellate cells in the anterior division of the anteroventral cochlear nucleus of the cat. Neuroscience 6:2643–2655.

Cant NB, Morest DK. 1979. The bushy cells in the anteroventral cochlear nucleus of the cat. A study with the electron microscope. Neuroscience 4:1925–1945.

Cant NB, Morest DK. 1979. Organization of the neurons in the anterior division of the anteroventral cochlear nucleus of the cat. Light-microscopic observations. Neuroscience 4:1909–1923.

Caspary DM, Backoff PM, Finlayson PG, Palombi PS. 1994. Inhibitory inputs modulate discharge rate within frequency receptive fields of anteroventral cochlear nucleus neurons. J Neurophysiol 72:2124–2133.

Caspary DM, Palombi PS, Hughes LF. 2002. GABAergic inputs shape responses to amplitude modulated stimuli in the inferior colliculus. Hear Res 168:163–173.

Caspary DM, Pazara KE, Kossl M, Faingold CL. 1987. Strychnine alters the fusiform cell output from the dorsal cochlear nucleus. Brain Res 417:273–282.

Coggeshall RE, Lekan HA. 1996. Methods for determining numbers of cells and synapses: a case for more uniform standards of review. J Comp Neurol 364:6–15.

Doucet JR, Ross AT, Gillespie MB, Ryugo DK. 1999. Glycine immunoreactivity of multipolar neurons in the ventral cochlear nucleus which project to the dorsal cochlear nucleus. J Comp Neurol 408:515–531.

Doucet JR, Ryugo DK. 1997. Projections from the ventral cochlear nucleus to the dorsal cochlear nucleus in rats. J Comp Neurol 385:245–264.

Francis HW, Manis PB. 2000. Effects of deafferentation on the electrophysiology of ventral cochlear nucleus neurons. Hear Res 149:91–105.

Gerken GM. 1979. Temporal summation of pulsate brain stimulation in normal and deafened cats. J Acoust Soc Am 66:728–734.

Godfrey DA, Farms WB, Godfrey TG, Mikesell NL, Liu J. 2000. Amino acid concentrations in rat cochlear nucleus and superior olive. Hear Res 150:189–205.

Golding NL, Oertel D. 1996. Context-dependent synaptic action of glycinergic and GABAergic inputs in the dorsal cochlear nucleus. J Neurosci 16:2208–2219.

Grothe B, Sanes DH. 1993. Bilateral inhibition by glycinergic afferents in the medial superior olive. J Neurophysiol 69:1192–1196.

Harty TP, Manis PB. 1998. Kinetic analysis of glycine receptor currents in ventral cochlear nucleus. J Neurophysiol 79:1891–1901.

Helfert RH, Juiz JM, Bledsoe SC Jr, Bonneau JM, Wenthold RJ, Altschuler RA. 1992. Patterns of glutamate, glycine, and GABA immunolabeling in four synaptic terminal classes in the lateral superior olive of the guinea pig. J Comp Neurol 323:305–325.

Holt AG, Asako M, Lomax CA, MacDonald J, Tong L, Lomax MI, Altschuler RA. 2005. Deafness related plasticity in the inferior colliculus: gene expression profiling following removal of peripheral activity. J Neurochem 93:1069–1086.

Juiz JM, Helfert RH, Bonneau JM, Wenthold RJ, Altschuler RA. 1996. Three classes of inhibitory amino acid terminals in the cochlear nucleus of the guinea pig. J Comp Neurol 373:11–26.

Kaltenbach JA. 2000. Neurophysiologic mechanisms of tinnitus. J Am Acad Audiol 11:125–137.

Kim JJ, Gross J, Morest DK, Potashner SJ. 2004a. Quantitative study of degeneration and new growth of axons and synaptic endings in the chinchilla cochlear nucleus after acoustic overstimulation. J Neurosci Res 77:829–842.

Kim JJ, Gross J, Potashner SJ, Morest DK. 2004b. Fine structure of degeneration in the cochlear nucleus of the chinchilla after acoustic overstimulation. J Neurosci Res 77:798–816.

Kim JJ, Gross J, Potashner SJ, Morest DK. 2004c. Fine structure of long-term changes in the cochlear nucleus after acoustic overstimulation: chronic degeneration and new growth of synaptic endings. J Neurosci Res 77:817–828.

Kolston J, Osen KK, Hackney CM, Ottersen OP, Storm-Mathisen J. 1992. An atlas of glycine- and GABA-like immunoreactivity and colocalization in the cochlear nuclear complex of the guinea pig. Anat Embryol (Berl) 186:443–465.

Krenning J, Hughes LF, Caspary DM, Helfert RH. 1998. Age-related glycine receptor subunit changes in the cochlear nucleus of Fischer-344 rats. Laryngoscope 108:26–31.

Kuwabara N, Zook JM. 1992. Projections to the medial superior olive from the medial and lateral nuclei of the trapezoid body in rodents and bats. J Comp Neurol 324:522–538.

Kuwabara N, Zook JM. 1999. Local collateral projections from the medial superior olive to the superior paraolivary nucleus in the gerbil. Brain Res 846:59–71.

Leake PA, Snyder RL, Rebscher SJ, Moore CM, Vollmer M. 2000. Plasticity in central representations in the inferior colliculus induced by chronic single- vs. two-channel electrical stimulation by a cochlear implant after neonatal deafness. Hear Res 147:221–241.

Lesperance MM, Helfert RH, Altschuler RA. 1995. Deafness-induced cell size changes in rostral AVCN of the guinea pig. Hear Res 86:77–81.

Milbrandt JC, Holder TM, Wilson MC, Salvi RJ, Caspary DM. 2000. GAD levels and muscimol binding in rat inferior colliculus following acoustic trauma. Hear Res 147:251–260.

Mossop JE, Wilson MJ, Caspary DM, Moore DR. 2000. Down-regulation of inhibition following unilateral deafening. Hear Res 147:183–187.

Muly SM, Gross JS, Morest DK, Potashner SJ. 2002. Synaptophysin in the cochlear nucleus following acoustic trauma. Exp Neurol 177:202–221.

Nagase S, Miller JM, Dupont J, Lim HH, Sato K, Altschuler RA. 2000. Changes in cochlear electrical stimulation induced Fos expression in the rat inferior colliculus following deafness. Hear Res 147: 242–250.

Nishiyama N, Hardie NA, Shepherd RK. 2000. Neonatal sensorineural hearing loss affects neurone size in cat auditory midbrain. Hear Res 140:18–22.

Ostapoff EM, Benson CG, Saint Marie RL. 1997. GABA- and glycine-immunoreactive projections from the superior olivary complex to the cochlear nucleus in guinea pig. J Comp Neurol 381:500–512.

Pasic TR, Moore DR, Rubel EW. 1994. Effect of altered neuronal activity on cell size in the medial nucleus of the trapezoid body and ventral cochlear nucleus of the gerbil. J Comp Neurol 348:111–120.

Pasic TR, Rubel EW. 1989. Rapid changes in cochlear nucleus cell size following blockade of auditory nerve electrical activity in gerbils. J Comp Neurol 283:474–480.

Pasic TR, Rubel EW. 1991. Cochlear nucleus cell size is regulated by auditory nerve electrical activity. Otolaryngol Head Neck Surg 104: 6–13.

Potashner SJ, Suneja SK, Benson CG. 2000. Altered glycinergic synaptic activities in guinea pig brain stem auditory nuclei after unilateral cochlear ablation. Hear Res 147:125–136.

Salvi RJ, Wang J, Ding D. 2000. Auditory plasticity and hyperactivity following cochlear damage. Hear Res 147:261–274.

Sato K, Kuriyama H, Altschuler RA. 1995. Expression of glycine receptor subunits in the cochlear nucleus and superior olivary complex using non-radioactive in-situ hybridization. Hear Res 91:7–18.

Shaddock Palombi P, Backoff PM, Caspary DM. 2001. Responses of young and aged rat inferior colliculus neurons to sinusoidally amplitude modulated stimuli. Hear Res 153:174–180.

Snyder RL, Vollmer M, Moore CM, Rebscher SJ, Leake PA, Beitel RE. 2000. Responses of inferior colliculus neurons to amplitude-modulated intracochlear electrical pulses in deaf cats. J Neurophysiol 84:166–183.

Subramani M, Morest DK. 2004. Neuronal plasticity in the cochlear nucleus following acoustic overstimulation in mouse. Assoc Res Otolaryngol Abs: p 249.

Suneja SK, Benson CG, Potashner SJ. 1998a. Glycine receptors in adult guinea pig brain stem auditory nuclei: regulation after unilateral cochlear ablation. Exp Neurol 154:473–488.

Suneja SK, Potashner SJ, Benson CG. 1998b. Plastic changes in glycine and GABA release and uptake in adult brain stem auditory nuclei after unilateral middle ear ossicle removal and cochlear ablation. Exp Neurol 151:273–288.

Suneja SK, Potashner SJ. 2003. ERK and SAPK signaling in auditory brainstem neurons after unilateral cochlear ablation. J Neurosci Res 73:235–245.

Syka J. 2002. Plastic changes in the central auditory system after hearing loss, restoration of function, and during learning. Physiol Rev 82:601–636.

Wenthold RJ. 1987. Evidence for a glycinergic pathway connecting the two cochlear nuclei: an immunocytochemical and retrograde transport study. Brain Res 415:183–187.

Wenthold RJ, Huie D, Altschuler RA, Reeks KA. 1987. Glycine immunoreactivity localized in the cochlear nucleus and superior olivary complex. Neuroscience 22:897–912.

Wickesberg RE, Oertel D. 1990. Delayed, frequency-specific inhibition in the cochlear nuclei of mice: a mechanism for monaural echo suppression. J Neurosci 10:1762–1768.

Wickesberg RE, Whitlon D, Oertel D. 1991. Tuberculoventral neurons project to the multipolar cell area but not to the octopus cell area of the posteroventral cochlear nucleus. J Comp Neurol 313:457–468.

Wickesberg RE, Whitlon D, Oertel D. 1994. In vitro modulation of somatic glycine-like immunoreactivity in presumed glycinergic neurons. J Comp Neurol 339:311–327.

Willott JF, Aitkin LM, McFadden SL. 1993. Plasticity of auditory cortex associated with sensorineural hearing loss in adult C57BL/6J mice. J Comp Neurol 329:402–411.

Willott JF, Lu SM. 1982. Noise-induced hearing loss can alter neural coding and increase excitability in the central nervous system. Science 216:1331–1334.

Willott JF, Turner JG. 2000. Neural plasticity in the mouse inferior colliculus: relationship to hearing loss, augmented acoustic stimulation, and prepulse inhibition. Hear Res 147:275–281.

Winsky L, Jacobowitz DM. 1995. Effects of unilateral cochlea ablation on the distribution of calretinin mRNA and immunoreactivity in the guinea pig ventral cochlear nucleus. J Comp Neurol 354:564–582.

Wu SH, Kelly JB. 1994. Physiological evidence for ipsilateral inhibition in the lateral superior olive: synaptic responses in mouse brain slice. Hear Res 73:57–64.

Wu SH, Oertel D. 1986. Inhibitory circuitry in the ventral cochlear nucleus is probably mediated by glycine. J Neurosci 6:2691–2706.

Zhang S, Oertel D. 1993. Tuberculoventral cells of the dorsal cochlear nucleus of mice: intracellular recordings in slices. J Neurophysiol 69: 1409–1421.

Zhang J, Suneja SK, Potashner SJ. 2003. Protein kinase C regulation of glycine and gamma-aminobutyric acid release in brain stem auditory nuclei. Exp Neurol 182:75–86.

Zheng L, Godfrey DA, Waller HJ, Godfrey TG, Chen K, Sun Y. 2000. Effects of high-potassium-induced depolarization on amino acid chemistry of the dorsal cochlear nucleus in rat brain slices. Neurochem Res 25:823–835.